Semiannual Technical Summary

Integrated Optical Circuits and Exploratory Materials Research

31 December 1975

Prepared for the Defense Advanced Research Projects Agency under Electronic Systems Division Contract F19628-76-C-0002 by

Lincoln Laboratory
MASSACHUSETTS INSTITUTE OF TECHNOLOGY
LEXINGTON, MASSACHUSETTS

The work reported in this document was performed at Lincoln Laboratory, a center for research operated by Massachusetts Institute of Technology. This work was sponsored by the Defense Advanced Research Projects Agency under Air Force Contract F19628-76-C-0002 (ARPA Order 2274); it is being monitored by the Rome Air Development Center.

This report may be reproduced to satisfy needs of U.S. Government agencies.

This technical report has been reviewed and is approved for publication.

FOR THE COMMANDER

William H. Lawton, Lt. Col., USAF
Acting Chief, ESD Lincoln Laboratory Project Office

MASSACHUSETTS INSTITUTE OF TECHNOLOGY
LINCOLN LABORATORY

INTEGRATED OPTICAL CIRCUITS AND EXPLORATORY MATERIALS RESEARCH

SEMIANNUAL TECHNICAL SUMMARY REPORT
TO THE
DEFENSE ADVANCED RESEARCH PROJECTS AGENCY

1 JULY – 31 DECEMBER 1975

ISSUED 19 JULY 1976

LEXINGTON MASSACHUSETTS

ABSTRACT

Two types of low-loss single-mode $p^+n^-n^+$ GaAs three-dimensional waveguides have been successfully fabricated and their attenuation coefficients measured. The devices are an optical stripline and a new device, the channel-stop strip guide. The channel-stop strip guides have losses of 0.8 cm^{-1} at 1.06 μm and 1.1 cm^{-1} at 0.920 μm; the losses for the optical striplines are 1.2 cm^{-1} at 1.06 μm and 1.7 cm^{-1} at 0.920 μm. A first-order loss calculation has yielded attenuation coefficients within 25 percent of these measured values. Both structures have an n^+ substrate, an n^- epitaxial layer for guiding, and p^+ regions to laterally confine the light. The p^+ regions have a uniform concentration and are formed by multiple-energy Be^+-ion implantation. The p^+n^- junctions show sharp high-voltage breakdowns at sufficiently high electric fields in the n^- layer (1.5×10^5 V/cm) to enable their use in directional-coupler switches and electroabsorption modulators.

The causes for reduced external quantum efficiencies in integrated etched-mesa GaAs-AlGaAs double-heterostructure (DH) lasers have been investigated. The primary loss mechanism appears to be the scattering of light by imperfections in the etched end mirrors.

As a first step in the investigation of heteroepitaxial growth with the aid of surface relief structures, a combination of laser holography and x-ray lithography techniques have been used to produce 3200 Å period gratings in photoresist. Straight edges and sharp vertical profiles were obtained in PMMA (polymethyl methacrylate) by soft x-ray lithography using holographically produced masks.

To investigate the potential of insulator-metal transitions for optical switching devices, thin-film VO_2 modulators have been fabricated and evaluated at submillimeter wavelengths. Modulation of about 70 percent was obtained in devices that were switched by electrical heating with response speeds on the order of 1 msec.

CONTENTS

INTEGRATED OPTICAL CIRCUITS AND EXPLORATORY MATERIALS RESEARCH

I. INTEGRATED OPTICAL CIRCUITS

A. LOW-LOSS GaAs $p^+n^-n^+$ THREE-DIMENSIONAL WAVEGUIDES

The development of GaAs-based integrated optical circuits (IOCs) requires low-loss three-dimensional waveguides. We have now successfully fabricated two types of single-mode $p^+n^-n^+$ three-dimensional guides entirely in GaAs; an optical stripline and a new device, the channel-stop strip guide. Both waveguides have an n^+ substrate, an n^- epitaxial region for guiding, and p^+ regions to laterally confine the light. The p^+ regions are formed by Be^+-ion implantation. The structures exhibit low optical loss (α as low as 0.8 cm^{-1} at 1.06 μm) and the p^+n^- junctions have sharp high-voltage breakdowns (corresponding to an average electric field in the n^- layer of 1.5×10^5 V/cm). Both types offer several advantages over other three-dimensional GaAs guides previously reported. In comparison to striplines with n^+ ribs,[1] these junction devices have a comparable or lower optical loss, and additionally allow high electric fields at low leakage currents to be applied to the guide by reverse-biasing the p^+n^- junction. This should facilitate the fabrication of modulators and switches using electroabsorption or electro-optic effects. Schottky-barrier devices,[2,3] which do permit electro-optical effects, and proton-bombarded embedded strips[4] have higher losses than these $p^+n^-n^+$ guides.

A cross-section sketch of an idealized optical stripline structure[5] is shown in Fig. 1(a), along with a sketch of the associated refractive index profile. The device consists of a rib of index n_3 over a slab of index n_2 and a substrate of index n_1. Region 4 is air. As indicated in the figure, the index of the slab is greater than that of the rib which in turn is larger than the substrate index. The effective guide index is largest under the rib, so that light propagating

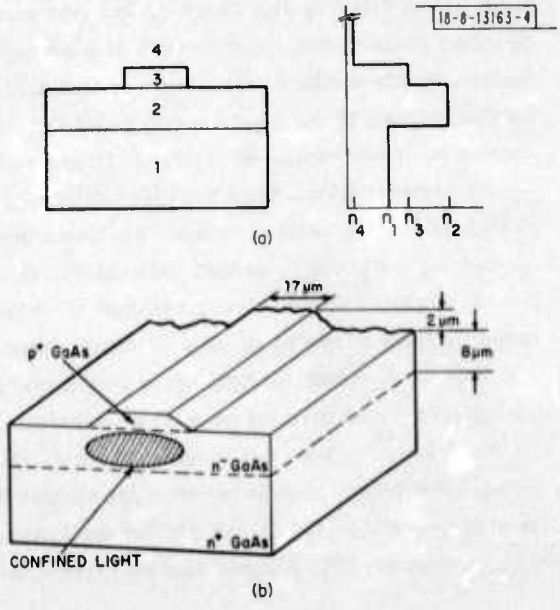

Fig. 1. (a) Schematic diagram of an optical stripline showing cross section of structure to the left and refractive index profile to the right. Region 4 is usually air. (b) Schematic diagram of a GaAs $p^+n^-n^+$ optical stripline showing propagating light confined in the n^- slab beneath the p^+ rib. Drawing is not to scale; dimensions refer to the single-mode device for which loss measurements are reported. Sloped sides of the rib result from the etching procedure used.

in the slab will be laterally confined there. Because the light is guided in the higher-index slab rather than in the rib, this device should have lower loss than some other rib structures,[6] since scattering losses due to rib edge roughness are minimized.

The stripline structure reported here, shown schematically in Fig. 1(b), was fabricated entirely in GaAs and consists of a p^+ rib, an n^- epitaxial layer, and an n^+ substrate. Devices were fabricated by first growing the undoped epitaxial layer by an $AsCl_3$-H_2-Ga vapor-phase technique on a (100)-oriented 1×10^{18} cm^{-3} n-type substrate. The layer was n-type, with a concentration of $\sim 1 \times 10^{14}$ cm^{-3}, a mobility at 77 K of 100,000 cm^2/V-sec, and a thickness of about 10 μm.

To form a p^+ layer, the sample surface was first encapsulated with ~700 Å of pyrolytic Si_3N_4 deposited at 720°C (Ref. 7). The epilayer was then implanted with Be^+ ions with doses of 1.5×10^{14} cm^{-2} at 400 keV, 1.2×10^{14} cm^{-2} at 220 keV, and 1.2×10^{14} cm^{-2} at 100 keV. Following the implant, the wafer was annealed at 900°C in flowing nitrogen for 15 minutes. Beryllium was chosen because it is the p-type dopant having the maximum penetration depth in GaAs; the multiple doses were chosen to create a heavily doped layer of uniform concentration and, thus, of uniform refractive index. Evaluation of this implantation technique by a series of etching steps and Hall measurements indicated that the implanted layers had a relatively constant p-type concentration of 2×10^{18} cm^{-3} to a depth of about 1.5 μm. The actual junction depth was found to be about 2 μm from the surface. Details of the Be^+-ion implantation and of the electrical characteristics of the p^+n^- junctions have been discussed elsewhere.[8] However, it should be noted here that ion implantation has several advantages for this doping task: it provided precise control on the depth and concentration of the implanted layer, and allows the option of selective doping by simple masking techniques.

After annealing, the Si_3N_4 encapsulation was removed in HF. Of the several procedures investigated to form the ribs, a Ti-masking technique was found to give the straightest and smoothest rib edges. In this method, stripes of several widths were defined along a $(0\bar{1}1)$ direction in a ~300-Å sputtered Ti layer by first patterning a photoresist film and then sputter-etching the exposed Ti. After the photoresist was removed, the GaAs was etched down through the p^+ layer (using the Ti as a mask) in a ~3°C solution of $1H_2SO_4$:$8H_2O_2$:$1H_2O$. For the orientation chosen, the sides of the ribs etched at a ~45° angle as indicated in Fig. 1(b). The finished devices had a rib height of 2 μm and an n^- layer thickness of 8 μm. The p^+n^- junctions formed by the isolated ribs and the undoped layer have shown sharp breakdowns at voltages corresponding to average electric fields in the punched-through n^- regions of 1.5×10^5 V/cm. Guides with rib widths from 10 to 35 μm were fabricated.

A cross-section sketch of the channel-stop strip guide is shown in Fig. 2(a) along with a sketch of the associated refractive index profile. The relative magnitude of the indices is given by $n_2 > n_3 > n_1 > n_4$. In this structure, the effective guide index is largest in the central portion of region 2 (between the regions of index n_3) and light will be guided there. The regions of index n_3 thus serve as optical-channel stops.

The GaAs channel-stop strip guide we have fabricated is shown schematically in Fig. 2(b). The guides were formed on wafers consisting of an n^- layer grown by vapor-phase epitaxy on a 1×10^{18} cm^{-3} n-type substrate. This n^- layer had a concentration of $\sim 1 \times 10^{14}$ cm^{-3} and was about 7 μm thick. Devices were fabricated by first depositing a 700-Å pyrolytic-Si_3N_4 film over the epitaxial layer. A photoresist layer of sufficient thickness to stop the Be^+ ions was then sprayed on the sample and patterned using standard techniques to form an implantation

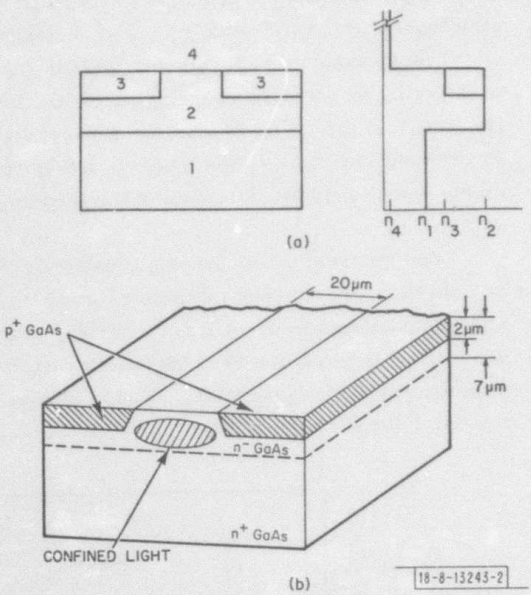

Fig. 2. (a) Schematic diagram of a channel-stop strip guide showing cross section of structure to the left and refractive index profile to the right. Region 4 is usually air. (b) Schematic diagram of a GaAs $p^+n^-n^+$ channel-stop strip guide showing propagating light confined in the n^- slab between the p^+ regions. Drawing is not to scale; dimensions refer to the single-mode device for which loss measurements are reported. Sloped sides of the p^+ regions result from the photoresist bombardment mask.

mask. The wafer was implanted with the same multiple doses used for the stripline. Following the implant, the photoresist was removed and the sample was annealed as described previously. The finished device had 2-μm-deep p-type regions. Structures having guiding-strip widths from 20 to 45 μm were fabricated. Relative to the rib-type guides, this structure has the advantages of being planar and easier to fabricate. Furthermore, since the light is guided between the p^+ regions, the channel-stop strip guide should minimize evanescent-tail losses and have lower attenuation for comparable optical confinement.

The mode characteristics of both the optical stripline and the channel-stop strip guide were calculated using the method of Marcatili.[9] These calculations indicate single-order-mode propagation for guiding widths less than ~26 μm for the stripline and ~35 μm for the channel-stop strip guide for the epitaxial-layer thicknesses in our devices. The observed modes are consistent with these computations. Figure 3 shows a photograph taken from a television monitor of the magnified image formed on an infrared vidicon of the near-field pattern at the output face of a single-mode channel-stop strip guide. The guiding region is about 20 μm wide and 7 μm high.

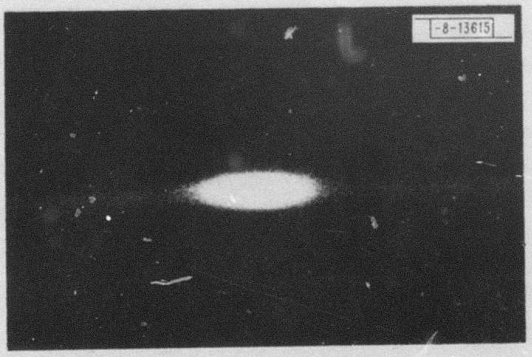

Fig. 3. Photograph of near-field intensity pattern at the output face of a single-mode channel-stop strip guide. Guiding region is about 20 μm wide and 7 μm high.

This single intensity maximum is typical of those observed. The E_{21}^{x} mode was observed on striplines with 35-μm-wide ribs and on channel-stop strip guides with 45-μm-wide guiding strips.

Transmission measurements on both the stripline and the channel-stop strip guide were made using an end-fire coupling scheme. The TE-polarized radiation from either a CW Nd:YAG laser at 1.06 μm or from a pulsed GaAs-GaAlAs DH stripe-geometry laser at 0.920 μm was focused on the cleaved input face of the guide using a microscope objective. The loss coefficients were found by determining the transmission through several lengths (≲1 cm) of the same sample.

Loss measurements on single-mode devices for the two $p^+n^-n^+$ structures are summarized in Table I. The guide width was 17 μm for the stripline and 20 μm for the strip guide. At 1.06 μm, the losses are 1.2 cm^{-1} for the stripline and 0.8 cm^{-1} (3.5 dB/cm) for the strip guide. We believe the loss for the channel-stop strip guide to be the lowest ever reported for a three-dimensional GaAs waveguide. The losses at 0.920 μm are 1.7 cm^{-1} for the stripline and 1.1 cm^{-1} for the strip guide.

TABLE I

MEASURED LOSS COEFFICIENTS FOR GaAs WAVEGUIDES

Device	Loss Coefficient (cm^{-1})*	
	λ = 1.06 μm	λ = 0.920 μm
Optical Stripline (17-μm-wide rib)	1.2	1.7
Channel-Stop Strip Guide (20-μm-wide strip)	0.8	1.1

*The uncertainty in the values is ±0.2 cm^{-1}.

A first-order loss calculation[10] yielded attenuation values within 25 percent of these measurement results. The calculation assumed that the optical power was confined to the central guiding region and thus modeled the devices as asymmetric slab waveguides; it was assumed that the stripline had a $p^+n^-n^+$ structure and that the channel-stop strip guide had an air-n^-n^+ structure. The absorption of the evanescent tails in the n^+ and p^+ regions as well as the residual absorption in the n^- guide were considered. In general, the calculated loss in the evanescent tails exceeded the residual guide loss deduced from measurements of thick planar GaAs waveguides.[11]

The low optical loss in conjunction with the good electrical characteristics of the p^+n^- junctions[8] suggests that these optical striplines and channel-stop strip guides are well suited for the development of GaAs modulators and switches using electro-optical effects, and would be useful in IOCs operating at GaAs-laser wavelengths.

F. J. Leonberger
J. P. Donnelly
C. O. Bozler

B. INTEGRATED GaAs-AlGaAs DH LASERS

In a previous report,[12] it was noted that the external differential quantum efficiencies of the integrated GaAs-AlGaAs DH lasers were somewhat lower (3.4 percent per end) than would be expected from results on typical cleaved DH lasers (10 to 20 percent per end). Further investigation has now indicated that the reduced efficiency is caused not by the presence of internally reflected circulating modes, as had been suspected, but more likely by scattering of light by imperfections in the etched end mirrors. These results are in essential agreement with those of others[13] on etched-mesa GaAs-AlGaAs DH lasers (18 percent maximum but 10 percent typical from both ends).

It was first established that inefficient coupling to the waveguide layer of the integrated device was not a causative factor by comparing the efficiencies of etched-mesa lasers before and after the growth of the waveguide. External efficiencies were essentially the same. In order to eliminate the possibility of internally reflected circulating or "bounce" modes, active stripes of widths 6, 12, and 25 μm were formed down the centers of the 100 μm wide by 310 μm long etched-mesa lasers. The technique of proton bombardment was employed to define the stripes and to render the portion of the mesa outside the stripe inactive.[14] The large optical absorption in this inactive region would then quench any modes utilizing the sides of the mesas as mirrors. Again, however, the quantum efficiencies of the stripe lasers were essentially the same as those of the broad-area etched mesas, indicating that the presence of circulating modes was not the cause of the low efficiencies.

A careful examination of the etched-mesa lasers using scanning electron microscopy indicated that on a microscopic scale the etched mirror faces of these lasers were much less smooth and flat than originally believed. Whereas smooth and highly perfect mesa faces, as shown in Fig. 4, could be routinely produced in bulk GaAs, the mesas etched into DH GaAs-AlGaAs wafers using the same masks and techniques were rough and non-flat. Figure 5 shows a typical example. A number of different etchants, including those of the $H_2SO_4:H_2O_2:H_2O$, $Br:CH_3OH$, and $CH_3OH:H_3PO_4:H_2O_2$ systems were tried, with little difference. The reason for the roughness is not known but must be due to imperfections or strains in the DH wafers and/or to the electrochemistry of etching in the presence of the potential variations of the heterojunctions.

It is believed that the reduced quantum efficiency of these lasers is due to scattering and reflection at incorrect angles from the rough mirrors. Side-by-side comparison of etched-mesa and normal cleaved lasers from the same wafer yield essentially identical threshold current densities but quantum efficiencies differing by factors of 4 to 6. It would be expected that somewhere along the etched faces would be at least one area of proper reflection to permit low threshold lasing in a filament, but that over most of the face light would be scattered or reflected improperly and lead to high optical losses and, hence, to low differential quantum efficiency. Although this limitation is not a fundamental one, at present the technique of etching more perfect faces has not been developed.

C. E. Hurwitz
J. A. Rossi

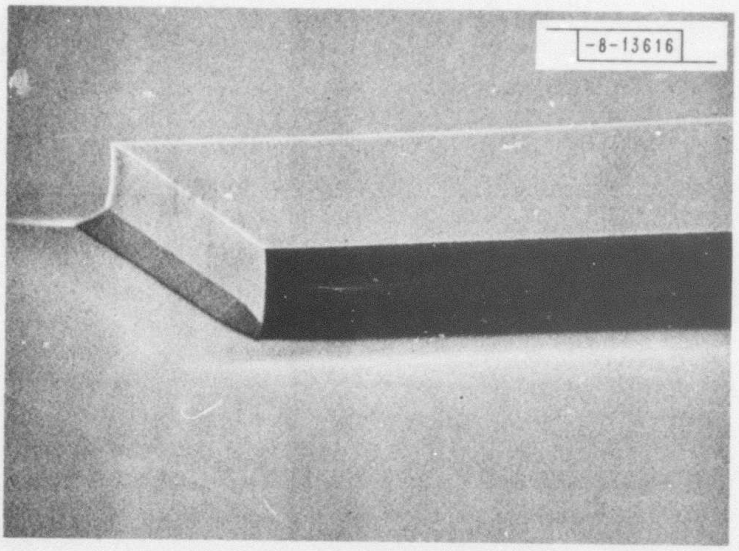

(a)

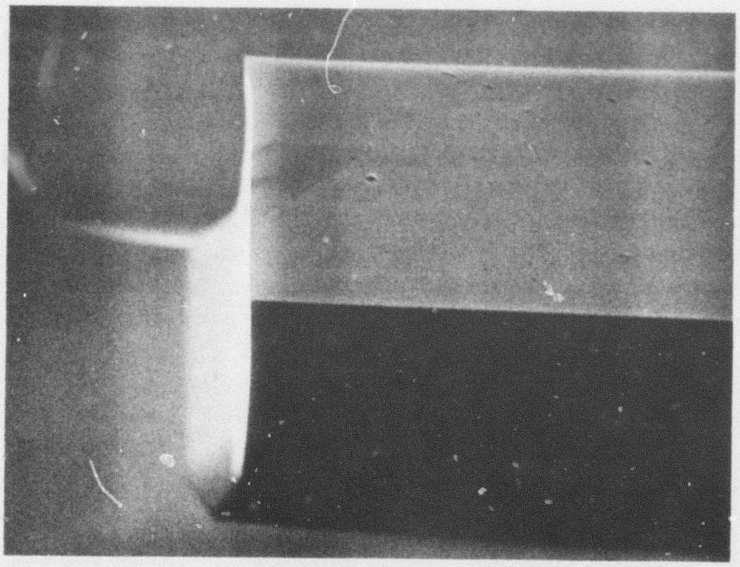

(b)

Fig. 4. SEM photograph of mesa etched into bulk GaAs. (a) Magnification 2000; (b) magnification 5000. Mesa faces are all (100).

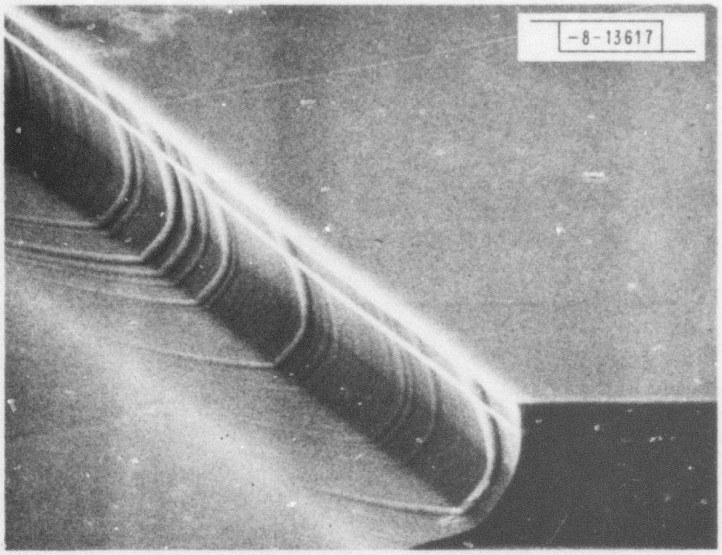

(a)

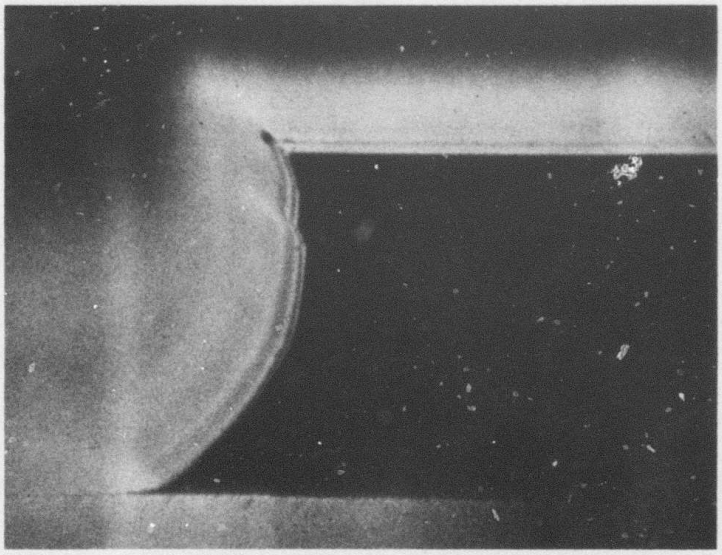

(b)

Fig. 5. SEM photograph of mesa etched into AlGaAs/GaAs DH wafer. (a) Magnification 2000; (b) magnification 5000. Mesa faces are all (100).

II. EXPLORATORY MATERIALS RESEARCH

A. ENHANCED HETEROEPITAXY

As a first step in a program aimed at determining the effect of high-resolution surface relief structures on heteroepitaxial growth, a laser holographic facility was established which permits the exposure of 3200-Å period gratings in photoresist. This facility was used to expose grating patterns on x-ray lithography masks. Gold absorber patterns on the mask were subsequently defined by ion beam etching. Figure 6 illustrates the straight edges and sharp vertical profiles that were obtained in PMMA by soft x-ray lithography using the holographically produced masks. The exposure time was 7 hours. Work was begun on new types of x-ray masks made from 1000-Å-thick silicon nitride membranes so that the exposure time could be reduced to about 15 minutes.

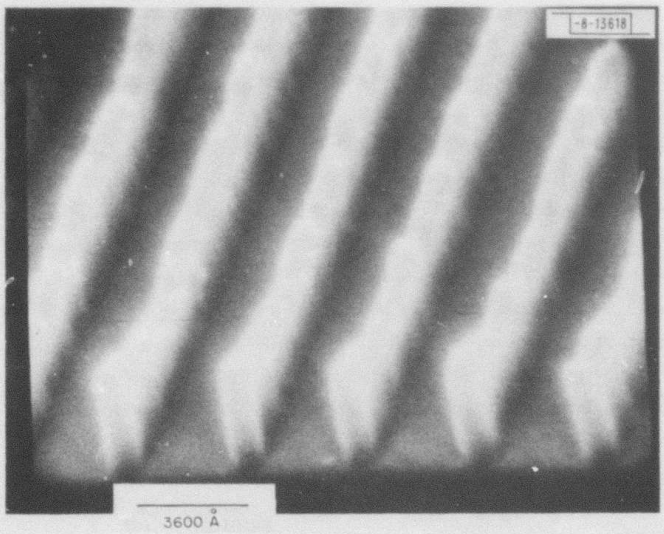

Fig. 6. Scanning electron micrograph of cross section of a grating pattern exposed in a PMMA film using soft x-ray (13.3 Å) lithography.

Scanning electron microscope studies of high-resolution relief structures ion-beam etched into surfaces showed that redeposition of sputtered material along polymer sidewalls poses a problem to etching sharp vertical steps. A number of approaches to solving this problem are being investigated.

H. I. Smith
D. C. Flanders

B. APPLICATIONS OF INSULATOR-METAL TRANSITIONS

A preliminary study of insulator-metal transitions has been undertaken to assess the potential for using such transitions in optical switching devices, including modulators and switchable diffraction gratings for use as variable-wavelength filters. Insulator-metal phase transitions are observed in certain compounds of the transition and rare-earth metals. At the transition temperature, the nature of the electrical conductivity of these compounds changes abruptly

from insulating to metallic. There is a corresponding change in optical properties. The optical changes are greatest in the infrared region where free electron absorption effects dominate when the material is in the metallic state. It is the large changes in the electrical and optical properties at the phase transition which make these compounds useful for applications in microelectronics and optoelectronics. There are over twenty compounds that exhibit insulator-metal transitions. We have concentrated on vanadium dioxide (VO_2), partly because it has a convenient transition temperature (~65°C), and partly because VO_2 has a fairly large transition – the electrical conductivity changing by as much as a factor of 10^5 in single crystals. This investigation describes the use of sputtered VO_2 thin films as optical switches at submillimeter wavelengths. It is expected that the results could be used to determine the feasibility of this class of devices at shorter infrared wavelengths.

Polycrystalline VO_2 films were deposited on single-crystal sapphire substrates by reactive sputtering a vanadium target in a mixture of Ar and O_2. Preparation of films with desired properties is made difficult by the existence of many different oxides in the vanadium-oxygen system.[15] The growth conditions were quite critical and have been described elsewhere.[16] The VO_2 films have a resistivity change in going from the insulating state to the metallic state of about 2×10^3 at 65°C.

Figure 7 shows a schematic drawing of the experimental setup. The 337-μm radiation is provided by a HCN laser and is measured by a GaAs photoconductive detector. Initially, we measured the optical transmission at 337 μm of a bare 0.6-mm-thick sapphire substrate, and of a 0.25-μm-thick VO_2 film on a sapphire substrate of the same thickness. Measurements were made with the film in both the high-resistivity and low-resistivity states. For these measurements, switching was accomplished by heating the film through the phase transition with a heater. The bare substrate transmits about 80 percent, while the VO_2 on sapphire has about the same transmission (within the experimental uncertainty of 5 percent) in the insulating state. In the metallic state, the free electron effects reduce the transmission to 25 percent, resulting in a relative change of about 70 percent.

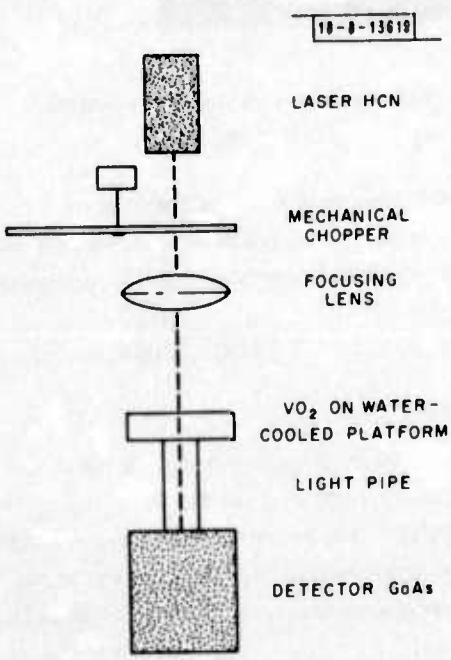

Fig. 7. Schematic representation of VO_2 optical modulation experimental setup.

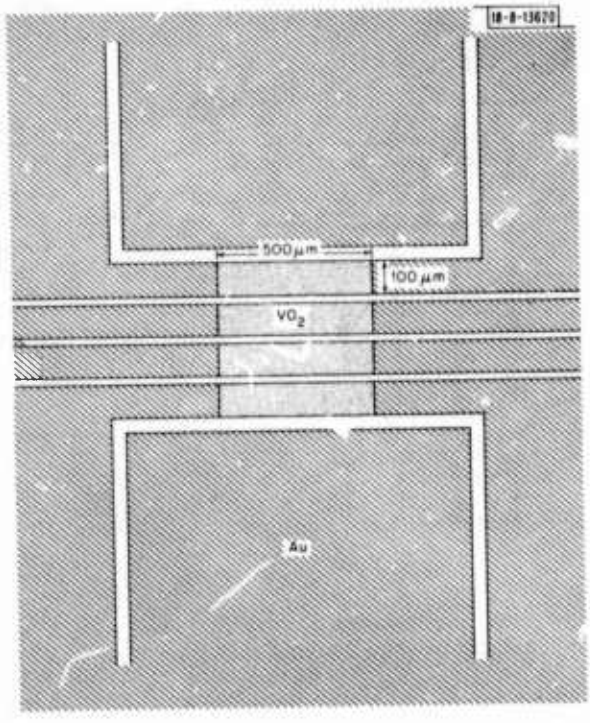

Fig. 8. Schematic diagram of VO_2 device configuration.

It is also possible to induce the optical switching by direct electric heating. Figure 8 shows the device configuration we used for the experiment. In this case, the VO_2 devices were fabricated by photolithographic techniques. Initially, four VO_2 elements of 100 by 700 μm were obtained by etching out a pattern from a continuous VO_2 film. The etchant used was 1:1 HNO_3:H_2O_2. Electrical contacts were then fabricated on these elements by the following procedure. A film of 500 Å of titanium followed by 3000 Å of gold was sputtered onto the VO_2 elements. The purpose of the titanium underlayer is to provide adhesion between the gold and the VO_2. After removal from the sputtering system, the substrates were coated with approximately 1.2 μm AZ 1350 photoresist. The desired device pattern was achieved by exposing the unwanted photoresist with ultraviolet radiation through an appropriate mask, removing the exposed resist followed by rinsing in deionized water and drying by N_2 gas. The exposed gold was then etched away using an iodine-based etchant and the thin titanium film exposed was etched in 20:1 H_2O:HF. (VO_2 is only slightly soluble in HF.) After etching, the substrate was rinsed in deionized water. The unexposed photoresist was then removed with acetone, and the substrates rinsed again in deionized water and finally dried with N_2. The resultant devices of dimensions 500 μm long and 100 μm wide are shown in Fig. 8; there are four devices. The open spaces in the figures are just bare substrates for electrical isolation and these spaces were blocked by gold stripes on the backside of the substrate to minimize leakage of light. The room temperature resistance was about 50 kohm and the resistance change at the phase transition is more than a factor of 10^2.

Using the electrical circuit shown in Fig. 9, the four VO_2 devices were switched on by a pulse generator with variable duty cycles. The duty cycles were adjusted for the maximum optical modulation. Figure 10(a) shows the detector signal before the VO_2 devices were switched on. When a voltage pulse train (160 V, 100 Hz) was applied to the four VO_2 devices, all four devices were switched on, as indicated by the small dots on the current pulses in Fig. 10(c). Figure 10(b) shows the detector signal when the VO_2 modulator was on. The laser radiation

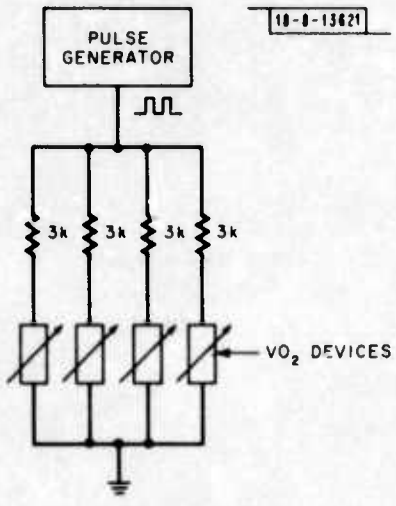

Fig. 9. Electrical circuit used for VO_2 experiment.

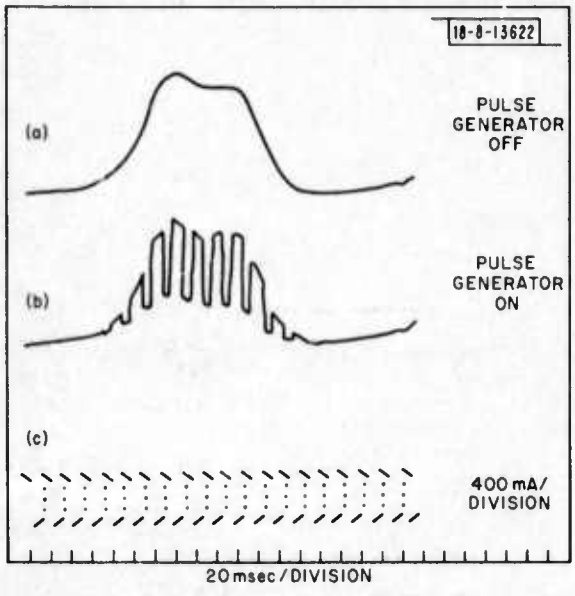

Fig. 10. Optical detector signal: (a) before VO_2 devices were switched on and (b) after VO_2 devices were switched on; (c) current pulses indicating that all four VO_2 devices were switched on and off.

was modulated about 70 percent, which is about the same depth of modulation when the devices were switched on by a heater. When the modulating frequency increased to 1000 Hz, the modulation magnitude decreased from 70 to 60 percent, indicating the response time of the VO_2 to the thermal cycle. When the frequency increased to 2000 Hz, the modulation decreased to 50 percent. The speed of the devices is limited by their cooling time, which is estimated about 1 msec under the operating conditions. If these devices were cooled to cryogenic temperatures, instead of just water-cooled, much greater speeds would be expected. Preliminary experiments indicate similar results for the 151-μm wavelength.

In conclusion, we have fabricated optical modulators for submillimeter wavelengths using VO_2 devices. Because the phase transition is a thermal process, the speed of modulation would be limited. Similar results are to be expected for 10 μm radiation, although we could not confirm this because of the sapphire-substrate absorption at 10 μm. For materials like Cr-doped V_2O_3, the observed insulator-metal transition has been suggested to be a Mott transition,[17] driven by electron-electron interactions which is a non-thermal process. If such a non-thermal switching is possible, much faster optical modulators could be fabricated.

J. C. C. Fan
H. R. Fetterman
F. J. Bachner
P. M. Zavracky
C. D. Parker

REFERENCES

1. H. Furuta, H. Noda, and A. Ithaya, Appl. Opt. 13, 322 (1974).
2. For a review, see H. Kogelnik, IEEE Trans. Microwave Theory Tech. MTT-23, 2 (1975).
3. F. A. Blum, D. W. Shaw, and W. C. Holton, Appl. Phys. Lett. 25, 116 (1974).
4. J. C. Campbell, F. A. Blum, and D. W. Shaw, Appl. Phys. Lett. 26, 640 (1975).
5. J. C. Campbell, F. A. Blum, D. W. Shaw, and K. L. Lamley, Appl. Phys. Lett. 27, 202 (1975).
6. S. Somekh, E. Garmire, A. Yariv, H. C. Garvin, and R. G. Hunsperger, Appl. Phys. Lett. 22, 46 (1973).
7. J. P. Donnelly, W. T. Lindley, and C. E. Hurwitz, Appl. Phys. Lett. 27, 41 (1975).
8. J. P. Donnelly, F. J. Leonberger, and C. O. Bozler (submitted to Appl. Phys. Lett.); J. P. Donnelly, F. J. Leonberger, and C. O. Bozler, Solid State Research Report, Lincoln Laboratory, M.I.T. (1976:1), pp. 8-11.
9. E. A. J. Marcatili, Bell Syst. Tech. J. 53, 645 (1974).
10. D. L. Spears, F. J. Leonberger, and S. R. Chinn (to be published).
11. G. E. Stillman, C. M. Wolfe, J. A. Rossi, and H. Heckscher, Appl. Phys. Lett. 28, 197 (1976).
12. Integrated Optical Circuits Semiannual Technical Summary, Lincoln Laboratory, M.I.T. (31 December 1974), p. 3, DDC AD-A014254/7.
13. J. L. Merz and R. A. Logan, Topical Meeting on Integrated Optics, Salt Lake City, 12-14 January 1976, Paper WC8-1.
14. J. C. Dyment et al., Proc. IEEE 60, 726 (1972).
15. K. Kosuge, J. Phys. Chem. Solids 28, 1613 (1967); J. B. MacChesney, J. F. Potter, and H. J. Guggenheim, J. Electrochem. Soc. 115, 82 (1968).
16. J. C. C. Fan and F. J. Bachner, Solid State Research Report, Lincoln Laboratory, M.I.T. (1972:3), p. 39, DDC AD-752556.
17. D. B. McWhan, T. M. Rice, and J. P. Remeika, Phys. Rev. Lett. 23, 1384 (1969); D. B. McWhan and J. P. Remeika, Phys. Rev. B2, 3734 (1970).

UNCLASSIFIED

SECURITY CLASSIFICATION OF THIS PAGE *(When Data Entered)*

REPORT DOCUMENTATION PAGE

READ INSTRUCTIONS BEFORE COMPLETING FORM

1. REPORT NUMBER
ESD-TR-76-117

2. GOVT ACCESSION NO.

3. RECIPIENT'S CATALOG NUMBER

4. TITLE (and Subtitle)
Integrated Optical Circuits and Exploratory Materials Research

5. TYPE OF REPORT & PERIOD COVERED
Semiannual Technical Summary
1 Jul[redacted] – 31 Dec[redacted]975

6. PERFORMING ORG. REPORT NUMBER

7. AUTHOR(s)
Ivars Melngailis

8. CONTRACT OR GRANT NUMBER(s)
F19628-76-C-0002

9. PERFORMING ORGANIZATION NAME AND ADDRESS
Lincoln Laboratory, M.I.T.
P.O. Box 73
Lexington, MA 02173

10. PROGRAM ELEMENT, PROJECT, TASK AREA & WORK UNIT NUMBERS
ARPA Order 2074
Program Element No. 61101E

11. CONTROLLING OFFICE NAME AND ADDRESS
Defense Advanced Research Projects Agency
1400 Wilson Boulevard
Arlington, VA 22209

12. REPORT DATE
31 Dec[redacted]975

13. NUMBER OF PAGES
20

14. MONITORING AGENCY NAME & ADDRESS *(if different from Controlling Office)*
Rome Air Development Center
Hanscom AFB
Bedford, MA 01731

15. SECURITY CLASS. *(of this report)*
Unclassified

15a. DECLASSIFICATION DOWNGRADING SCHEDULE

16. DISTRIBUTION STATEMENT *(of this Report)*

Approved for public release; distribution unlimited.

17. DISTRIBUTION STATEMENT *(of the abstract entered in Block 20, if different from Report)*

18. SUPPLEMENTARY NOTES

None

19. KEY WORDS *(Continue on reverse side if necessary and identify by block number)*

integrated optical circuits	epitaxial growth	heteroepitaxy
GaAs	ion implantation	insulator-metal transitions
optical waveguides	lasers	optical switches

20. ABSTRACT *(Continue on reverse side if necessary and identify by block number)*

Two types of low-loss single-mode $p^+n^-n^+$ GaAs three-dimensional waveguides have been successfully fabricated with attenuation coefficients of 0.8 cm^{-1} and 1.2 cm^{-1} at 1.06 μm. The reduced external quantum efficiencies in integrated etched-mesa GaAs-AlGaAs DH lasers have been shown to be primarily due to scattering of light by imperfections in the etched end mirrors.

As a first step in the investigation of heteroepitaxial growth with the aid of surface relief structures, a combination of laser holography and x-ray lithography techniques have been used to produce high-quality 3200 Å period gratings in photoresist.

To investigate the potential of insulator-metal transitions for optical switching devices, thin-film VO_2 modulators have been fabricated and evaluated at submillimeter wavelengths.

DD FORM 1 JAN 73 1473 EDITION OF 1 NOV 65 IS OBSOLETE

UNCLASSIFIED

SECURITY CLASSIFICATION OF THIS PAGE *(When Data Entered)*